[18] P. J. Huber, *Robust Statistics*, 1st ed. New York: Wiley, 1981.
[19] W. H. Press, S. A. Teukolsky, W. T. Vetterling, and B. P. Flannery, *Numerial Recipes in C: The Art of Scientific Computing*, 2nd ed. Cambridge, U.K.: Cambridge Univ. Press, 1992.

Control of Cooperating Mobile Manipulators

Thomas G. Sugar and Vijay Kumar

***Abstract*—We describe a framework and control algorithms for coordinating multiple mobile robots with manipulators focusing on tasks that require grasping, manipulation and transporting large and possibly flexible objects without special purpose fixtures. Because each robot has an independent controller and is autonomous, the coordination and synergy are realized through sensing and communication. The robots can cooperatively transport objects and march in a tightly controlled formation, while also having the capability to navigate autonomously. We describe the key aspects of the overall hierarchy and the basic algorithms, with specific applications to our experimental testbed consisting of three robots. We describe results from many experiments that demonstrate the ability of the system to carry flexible boards and large boxes as well as the system's robustness to alignment and odometry errors.**

***Index Terms*—Compliance, locomotion and grasping, mobile robot cooperation.**

I. Introduction

We address the coordination of a small team of mobile manipulators that cooperatively perform such manipulation tasks as grasping a large, flexible object and transporting it in a two dimensional environment with obstacles. Such a system of robots is useful in material handling applications where there are no special purpose material handling devices (for example, conveyors, fixtures or pallets are not present). In particular, when the team is remotely controlled or supervised, the system can be used for the clean-up of hazardous waste material [1].

We focus on tasks that simply cannot be performed by a single mobile robot. As examples, consider the transportation of the large box or the flexible board shown in Fig. 1. The object, a box or a flexible board in our experiments, is large enough that one platform cannot carry it by itself without expensive, special purpose tooling that is specific to the object. In our approach, two or more robots are coordinated to accomplish the task of carrying an object. We demonstrate four key features of our system: (a) coordination and cooperation between tightly coupled mobile robots; (b) palm-like grasping of an object; (c) decentralized control of cooperating robots; and (d) robust grasping and transportation.

The physical interaction between the robots and the tight coupling required of autonomous controllers pose many challenging engineering problems including:

1) the manipulators must be capable of controlling the grasp forces in a robust fashion;
2) there needs to be an efficient way of communicating and sharing information in real time;
3) it should be possible to organize the robots differently for different tasks forcing the controllers to be independent and yet able to function in a tightly coupled architecture when carrying objects;
4) the robots must coordinate their trajectories in order to maintain a desired formation while maintaining the grasp; Unlike the task of pushing a box, the robots must maintain a formation while grasping and *carrying* the object;
5) the team must be robust with respect to errors that include robot positioning errors and modeling errors.

There is extensive literature on the subject of coordinating a group of robots. The behavior based control paradigm of [2]–[4] has been shown to be successful in controlling a large team of loosely coupled robots. It is possible to synthesize an impressive array of group behaviors [5] and coordinate robots for tasks like cooperative pushing [6]–[8], clustering in formations [9] and exploration [10] using variations of this basic approach. However, it is not clear that this approach can be used in its current form to maintain a tight formation and control grasp forces for holding and transporting objects.

When two or three robots are tightly coupled together in a specified formation for a specified manipulation task, the control problem is well-defined and the feedback control laws for coordinating a small team of robots are reasonably well understood [11]–[13]. The feedback laws for coordinated control of manipulation and locomotion are discussed by [14], [15]. Our work differs from such approaches in three respects.

In contrast to approaches in which the planning and control problems for the multirobot team are done centrally [16], our goal is to decentralize the control and planning to the extent possible. Our approach to decentralized control relies on the *decoupling* of the subproblems of controlling locomotion and manipulation [11], [17]. Second, our formulation will allow for changes in formation, as well as changes in the composition of the team. Third, our formulation allows for a small number of robots, although there are many unresolved questions about the optimal organization of large teams of robots.

Finally, it is important to note that our method for decoupling the control issues in manipulation and locomotion relies on a novel manipulator design. Ideally, we want each mobile manipulator to be equipped with an end effector that allows it to exert controlled forces and moments on the object and can accommodate small position and orientation errors resulting from the use of nonholonomic robots. However, the control of contact forces and moments is well known to be notoriously difficult [18]. We propose a parallel manipulator design in which the control of contact interactions are accomplished via a set of inexpensive position controlled motors. Further, as shown in the paper, we will only require one of the two or three team members to be equipped with an actively controlled end effector. While the details of the design of the manipulator are available elsewhere [19], we will review the basic principles in as much as they relate to the performance of the system.

An overall framework for the system is described. The experimental system and control architecture is given next. Finally, multiple experiments are presented that demonstrate the ability of our system to transport different objects.

II. The Team of Robots

A. Organization

In this section, we briefly discuss the organization of the team of mobile manipulators and outline the basic assumptions for this work. We

Manuscript received September 25, 2000; revised August 23, 2001. This paper was recommended for publication by Associate Editor L. Kavraki and Editor I. Walker upon evaluation of the reviewers' comments.

T. G. Sugar is with the Department of Mechanical and Aerospace Engineering, Arizona State University, Tempe, AZ 85287 USA (e-mail: thomas.sugar@asu.edu.).

V. Kumar is with the GRASP Laboratory, University of Pennsylvania. Philadelphia, PA 19104-6228 USA.

Publisher Item Identifier S 1042-296X(02)01375-7.

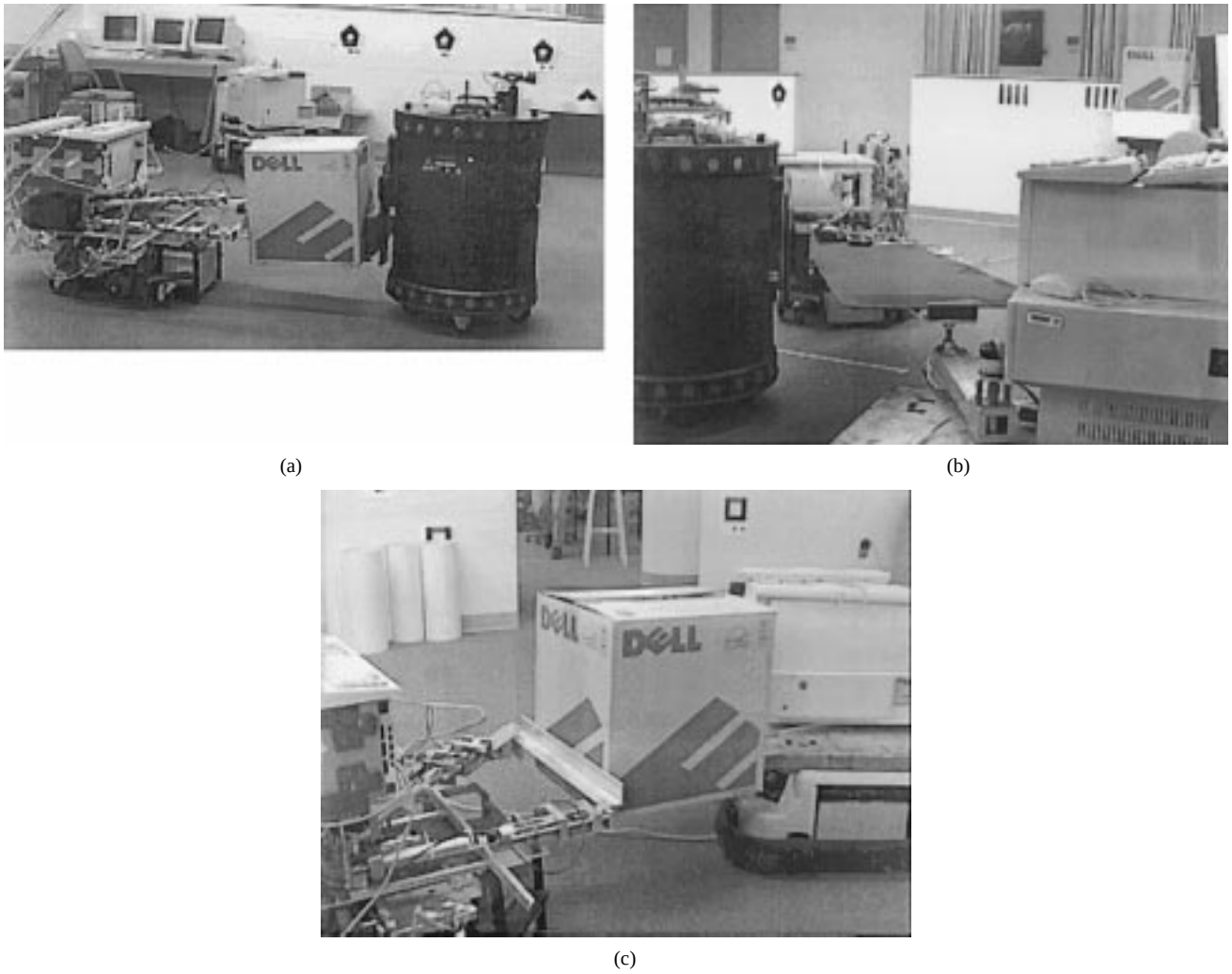

Fig. 1. Experimental system. (a) Our experimental testbed of two cooperating mobile manipulators. The robot to the right is the nomad XR4000 with a fork-lift. On the left is a TRC labmate platform equipped with the three degree-of-freedom compliant arm. (b) Three robots carrying a flexible board. The one to the right is the TRC platform with the stiff, passive, one degree-of-freedom arm. (c) Two TRC platforms that are both nonholonomic carrying an object.

will also review the "information structure" for the team, by listing the task specifications known to all the team members and the information that is exchanged between them during the task.

Our system of cooperating manipulators consists of two or three mobile manipulators. The tasks considered here involve picking up a large object and transporting it cooperatively in a two-dimensional environment. The control and coordination of the team is based on the following key ideas.

- Each robot is controlled independently so that the robots can be autonomous and it is possible to add or subtract team members.
- The team has one leader that plans the trajectory for the specified task. The leadership can be transferred from one robot to another robot during the task but at all points, one robot is designated as the leader. In a teleoperated system, this plan for the leader can be prescribed by a remotely located human operator.
- Cooperation is achieved by allowing the robots to share information. The leader shares only its trajectory with the followers and the followers broadcast critical information about the task.

The organization of the team is described by the identification of the labels R_1, R_2, and R_3 to the robots. R_1 is the leader as shown in Fig. 2. The team is described by the relative position and orientation of the robots in the team, the geometry of the grasped object and the kinematics of each robot. See Fig. 2. For every pair (R_i, R_j) of team members, the coordinates (r_{ij}, ψ_{ij}) specifying the relative position and orientation and the grasp force f_{ij} are known in the appropriate coordinate system. The mathematical modeling of a team of an arbitrary number of robots is discussed in [20], [21].

Two possible organizations of robots into teams are shown in Fig. 2. In each case, the lead robot, R_1, plans a trajectory for the formation based on sensory information. It is also incorporates constraints on the entire system, including nonholonomic constraints of the individual platforms. The plan generated by the lead platform is based on the knowledge of the kinematics of each team member and is broadcast to all the team members at frequent intervals. The rear platforms, R_2 (and R_3), receive the broadcast information from the lead platform and plan accordingly. Similarly, a force closure analysis yields an optimal distribution of forces. Each robot-object contact is a line contact, which can be modeled by a combination of normal and tangential forces and a moment about a convenient reference point. If the object geometry and weight and the coefficients of friction between the object and the effectors are known, the required internal forces[1] for a robust, force-closed grasp can be easily determined [23].

Each individual robot planner and controller are based on the following information:

[1]The *internal forces* [22], also sometimes called the *interaction forces* or the *squeeze forces*, are the contact forces lying in the nullspace of the grasp matrix.

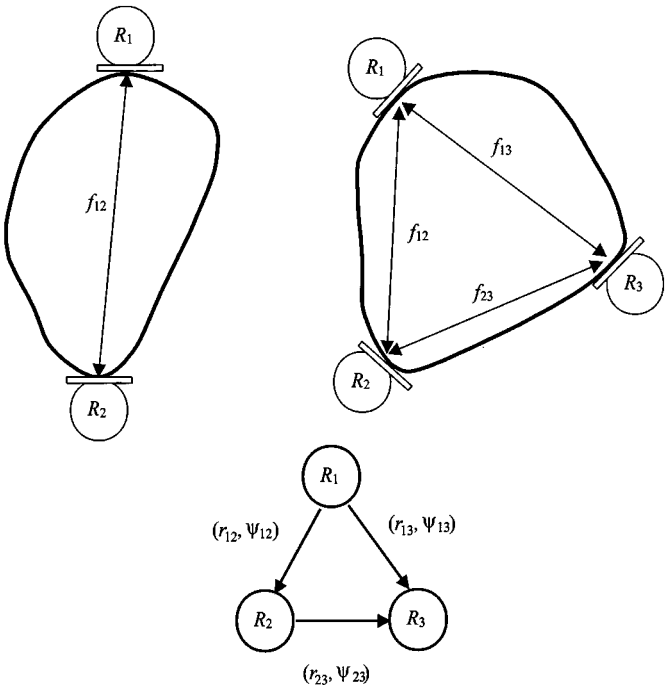

Fig. 2. The robot teams consisting of two or three robots. R_1 is the leader, while R_2 and R_3 are followers. R_1 broadcasts its trajectory at intervals based on information available from its sensors and a gross model of the team of robots, while the followers plan trajectories based on the broadcast plans, the sensory information available to them and their kinematic and dynamic constraints. The internal forces are specified by R_1, but the control of the forces and the trajectory does not rely on any exchange of information between the robots.

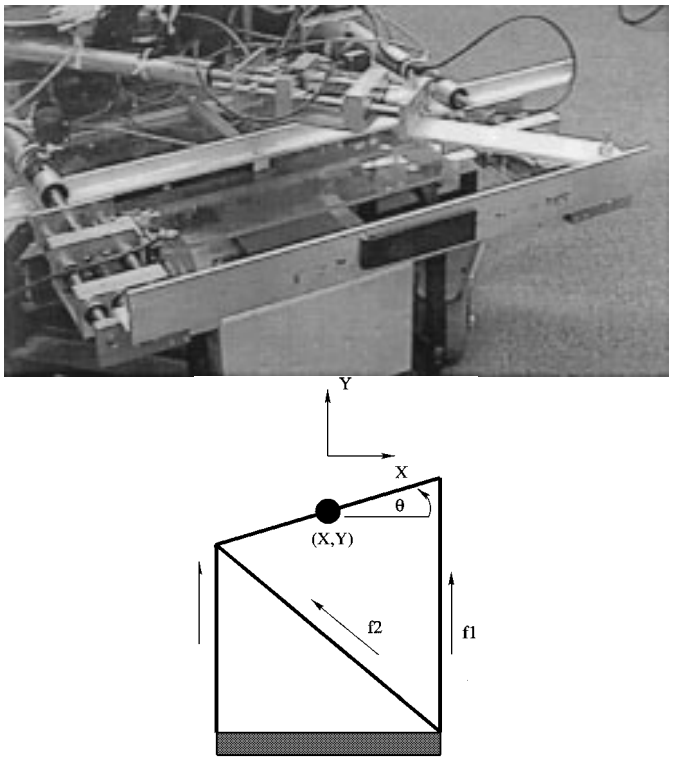

Fig. 3. The three degree-of-freedom, in-parallel, actively controlled arm applies a force in the X and Y directions as well as a moment in the Z direction. Each limb has a spring attached in series to a linear actuator driven by a dc motor attached to a ball screw transmission.

- The desired position, r_{1i} and orientation ψ_{1i} of the robot R_i relative to the leader R_1.
- The desired internal force f_{1i} that is required to be exerted for force closure.

Finally, each mobile manipulator is assumed to be able to maintain the desired position and orientation and control the contact forces. Each robot platform is able to control its trajectory through a velocity controller. If the robot platform has an actively controlled arm, it explicitly controls the internal force. If the robot platform has a passive arm as is the case with two of the three robots in Fig. 1, this force is not controlled. Instead, the robot acts as a very stiff position controlled effector.

B. Controlling the Manipulation and Locomotion Subsystems

The task for the lead robot is to follow its planned trajectory. The task for each follower robot is to follow the lead robot while maintaining the required grasp forces. In all cases, the controller for the manipulation and the locomotion systems have to be coordinated.

We decompose the planning and control system for each robot into three subsystems.

1) Planner : The trajectory for the lead robot can be based on any number of approaches that have been suggested for planning motions for a formation of robots [16], [24], [25]. This is not the main focus of this paper and is not addressed here. The planner for a follower robot "listens" to the information broadcast from the lead robot, gets information from its sensors and plans an appropriate reference trajectory that avoids obstacles. It provides set points for the mobile robot controller (a reference trajectory) and for the manipulator controller (grasp forces). The reference trajectory is consistent with the geometry of the formation, the (possibly) nonholonomic kinematic constraints and the broadcast plan of the leader [26].

2) Mobile Robot Controller: The controller insures that the robot will follow the specified reference trajectory. It computes the velocities for the drive motors. the reference trajectory provides the feedforward component. The feedback is provided by a *Look-ahead Controller* which compensates for errors due to arm movements and insures that the arm does not extend past its workspace boundary. More details can be found in Section II-C.

3) Arm Controller: The arm senses and controls the grasp forces, according to specifications transmitted from the lead robot. the active controlled arm used in our system is a three degree-of-freedom, in-parallel manipulator shown in Fig. 3. Each leg is driven by a simple position controlled motor in series with a linear spring [19]. By controlling the free length of the spring, it is possible to implement a stiffness control law that compensates for platform positioning errors while maintaining prescribed internal forces. Of course this is possible only for the active arm.

The active manipulator can be controlled by a stiffness control law that is of the form:

$$f = f_{\text{preload}} + K\,(x_0 - x_i) \tag{1}$$

where f is the force applied by the robot effector, K is the desired 3×3 Cartesian stiffness matrix associated with the effector and x_i is the 3×1 Cartesian position vector that represents the position and orientation of the reference frame $\{F_{i,0}\}$ attached to the effector relative to the reference frame attached to the grasped object, $\{F_i\}$. See Fig. 4. $f_{preload}$ and x_0 are the desired preload and the desired relative position (and orientation), respectively. The details of the control scheme that implements a stiffness controller are provided in [26]. The bandwidth for the arm interacting with an object is approximately 5 Hz.

When the arm is force controlled, the arm maintains a prescribed force f_{des}. The details of the implementation and experimental results demonstrating a control bandwidth of 24 Hz. are described in [26].

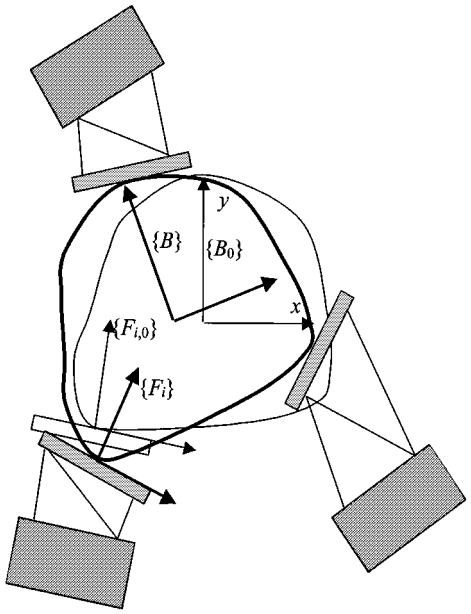

Fig. 4. $\{B\}$, the body fixed frame has moved from its initial position, $\{B_0\}$. Similarly, the reference frame, $\{F_i\}$, attached to the ith contact, has moved from its initial position, $\{F_{i,0}\}$.

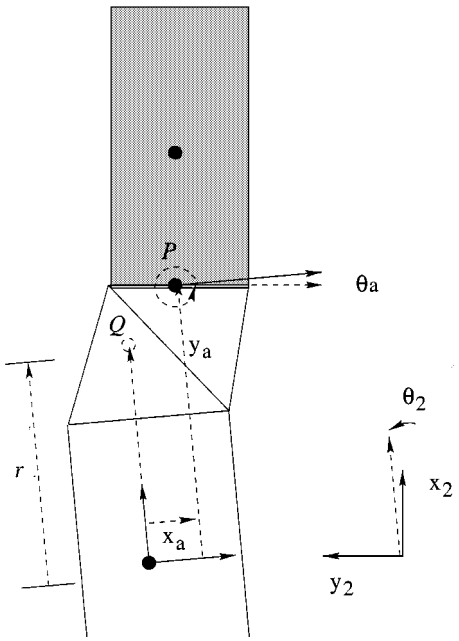

Fig. 5. Coordinate system for the controller.

C. Compensation for Errors

The computation of the platform reference trajectory by the planner which we have just described in the previous section, constitutes the feedforward commands for the platform controller. However, as described earlier, it is necessary to compensate for the arm movements so that the arm never reaches a state of complete extension or retraction. This *platform feedback compensation* law is discussed next. The controller compensates for odometry errors and the system can move 10 meters instead of less than 1 meter before the drift needs to be canceled.

Consider the two-platform configuration shown in Fig. 1(c) in which the lead robot has a stiff arm and the follower has the compliant arm. The positions and orientations of the lead platform and that of the follower platform are given in some fixed coordinate system by (x_1, y_1, θ_1) and (x_2, y_2, θ_2), respectively. The position and orientation of the arm end effector in a coordinate system attached to the follower are given by (x_a, y_a, θ_a) as shown in Fig. 5.

We are interested in maintaining the arm position and orientation so that the reference point (geometric center) on the end effector is at the center of the workspace. In other words, the desired operating point corresponds to point Q, with coordinates (z_1, z_2). The actual position of the center is denoted by point P, with coordinates (p_1, p_2). The controller of the follower platform attempts to make points P and Q coincide. In other words, Q can be thought of as a reference point on the platform, henceforth called the *look-ahead point* and the actual position of Q is given by P. Writing the expressions for the coordinates is simple:

$$z_1 = x_2 + r\cos\theta_2 \tag{2}$$

$$z_2 = y_2 + r\sin\theta_2. \tag{3}$$

The actual operating point of the tip of the arm is given by the coordinates of p_1 and p_2. The measurements, x_a and y_a, are calculated from the actively controlled compliant arm.

$$p_1 = x_2 + x_a\sin\theta_2 + y_a\cos\theta_2 \tag{4}$$

$$p_2 = y_2 - x_a\cos\theta_2 + y_a\sin\theta_2 \tag{5}$$

We want the look-ahead point, Q, to coincide with the point P. This suggests a control law that will result in the following behavior:

$$\dot{z}_1 = -K(z_1 - p_1) \tag{6}$$

$$\dot{z}_2 = -K(z_2 - p_2). \tag{7}$$

By differentiating (2)–(3) and substituting for $\dot{x}_2$, $\dot{y}_2$, and $\dot{\theta}_2$, in terms of the inputs v_2 and ω_2, we get:

$$\begin{pmatrix} \cos\theta_2 & -\sin\theta_2 \\ \sin\theta_2 & \cos\theta_2 \end{pmatrix} \begin{pmatrix} v_2 \\ r\omega_2 \end{pmatrix} = \begin{pmatrix} K\,(x_a\sin\theta_2 + y_a\cos\theta_2 - r\cos\theta_2) \\ K\,(-x_a\cos\theta_2 + y_a\sin\theta_2 - r\sin\theta_2) \end{pmatrix} \tag{8}$$

since

$$\begin{pmatrix} \dot{x}_2 \\ \dot{y}_2 \\ \dot{\theta}_2 \end{pmatrix} = \begin{pmatrix} \cos\theta_2 & 0 \\ \sin\theta_2 & 0 \\ 0 & 1 \end{pmatrix} \begin{pmatrix} v_2 \\ \omega_2 \end{pmatrix}. \tag{9}$$

Inverting the coefficient matrix which is orthogonal and never singular, we get the following control law:

$$\begin{pmatrix} v_2 \\ r\omega_2 \end{pmatrix} = \begin{pmatrix} K(y_a - r) \\ -K(x_a) \end{pmatrix}. \tag{10}$$

The control law or *look-ahead controller* is then used to modify the reference trajectory. Thus, the reference trajectory is modified only if there are errors in the arm positions which result from odometry errors, initial orientation errors, errors in the knowledge about the size of the box, or errors due to the robots not accelerating/decelerating in unison.

III. Experimental System

A. The Robots

The team currently consists of any combination of two or three robots. The three robots in our experimental system are shown in Fig. 1.

1) Robot A : A Nomad XR4000 platform equipped with a stiff fork-lift arm that has one prismatic joint along a vertical axis. In Fig. 1(a), it is the lead robot (R_1) and in Fig. 1(b) it is a follower (R_3).

This robot is completely designed and built by Nomadic Technologies, Inc. [27].

2) Robot B : A TRC Labmate platform equipped with an actively controlled compliant arm. The arm is shown in Fig. 3. The robot is used as a follower (R_2) in Fig. 1(a)–(c).

3) Robot C : A TRC Labmate platform equipped with a passive stiff arm with one revolute joint. It is used as a lead robot (R_1) in Fig. 1(c).

Each robot has two control computers, one for the locomotion subsystem and one for the manipulation subsystem. As discussed in the previous section, the locomotion system for each robot is position controlled to a planned trajectory. The control of the manipulator is done differently in the three robots. But in each case, it is independent from the locomotion controller. However, data from the manipulation controller is shared with the locomotion controller as inputs to the *look-ahead* controller. The actively controlled arm uses a force or stiffness controller and accommodates platform positioning errors. The controller for the passive arm simply monitors the state of the arm.

B. Communication

Our complex system with multiple mobile platforms and arms must be coordinated and controlled with a predictable performance. The key to this is a reliable system for communication.

Proxim Range LAN2 ISA wireless Ethernet boards [28] are used with the IPX (Internetwork Packet Exchange) protocol by all robots. We chose IPX because it is a very fast protocol (up to 80 packets a second) with the ability to send small packets (up to 576 bytes). This connectionless protocol makes the most sense for fast real time communication because small packets can be sent quickly.

IPX is a connectionless protocol based on a peer to peer network. The network is setup by creating a packet and physically sending it out by calling a hardware interrupt. We create our own packet and send it out by calling a hardware interrupt at a fixed rate. This fixed rate, although chosen very conservatively, guarantees a fixed communication bandwidth, which in turn is necessary for predictable real-time performance.

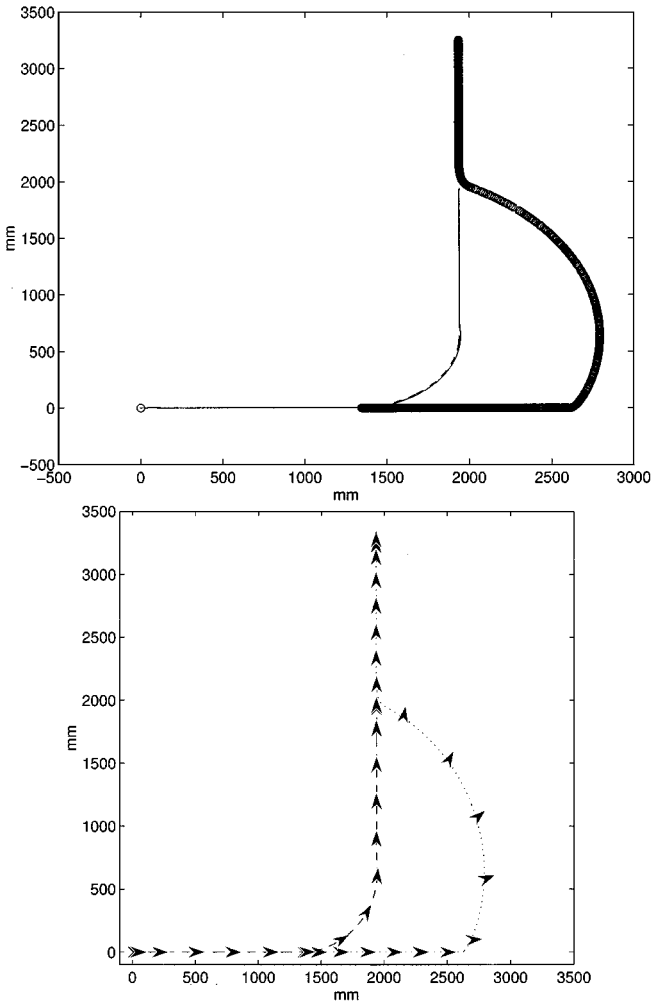

Fig. 6. Two robots carrying an object in the configuration shown in Fig. 1(a). The actual (solid, thick) path of Robot 1 and the desired (dashed) and actual (solid, thin) paths of Robot 2 are shown for Experiment 1. In the bottom figure, the orientations of the robots are shown by the arrows in addition to the actual path of Robot 1 (dotted) and Robot 2 (dashed).

IV. Experiments

In this section, we present detailed experimental results that substantiate the architecture and algorithms presented earlier. All the experiments are carried out with the robots shown in Fig. 1. Since the focus is on coordinated control of the cooperative manipulation task, all the experiments involve two or three robots handling a grasped object. Although the system is capable of approaching a designated object and picking up the object autonomously [26], [29], we will focus on the experimental results when grasping the object. The object in question is either a 0.5 m $\times$ 0.57 m $\times$ 0.7 m., 25 N box, or a a 0.5 m $\times$ 1.5 m $\times$ 0.005 m, 2 N flexible board. In both cases, as explained later, a model of the object is implicitly incorporated into the task specifications. More specifically, the inputs to the system are the relative position and orientation of each robot with respect to the leader, the desired internal forces and the desired Cartesian stiffness matrix. In at least one set of experiments, the effect of modeling errors is investigated.

A. Experiments With Two Mobile Manipulators

In this subsection, we present results from two different experiments with two robots carrying a large box as shown in Fig. 1(a). Robot 1 is the Nomad omnidirectional robot with a stiff, passive arm, while Robot 2 is a nonholonomic platform with an actively controlled compliant arm. In both experiments, the lead robot (Robot 1) follows a desired trajectory while the rear platform (Robot 2) follows while maintaining the desired formation. The arm controller is a stiffness controller in Experiment 1, while a pure force controller is used in Experiment 2.

The experiments are started with both robots aligned with their orientations at zero degrees, $r_{12} = 1.3$ m., $\psi_{12} = 0$ degrees. This translates to $\theta_1 = 0$ and $\theta_2 = 0$ in Fig. 1(a).

The desired (planned) and actual paths for the two platforms are shown in Fig. 6 (top) for Experiment 1. The desired and planned paths overlap making them virtually indistinguishable. Snapshots of the individual robots are shown in Fig. 6 (bottom). The trajectories in Experiments 1 and 2 are similar and the history of positions and orientations from Experiment 1 are only shown.

In Experiment 1, the home or the nominal position and orientation of the actively controlled arm is $x_a = 254$ mm, $y_a = 568$ mm, and $\theta_a = 0$. The arm is controlled using a stiffness control law and the commanded stiffness is

$$K = \begin{pmatrix} 350\ \frac{\text{N}}{\text{m}} & 0 & 0 \\ 0 & 525\ \frac{\text{N}}{\text{m}} & 0 \\ 0 & 0 & 90\ \text{Nm} \end{pmatrix}$$

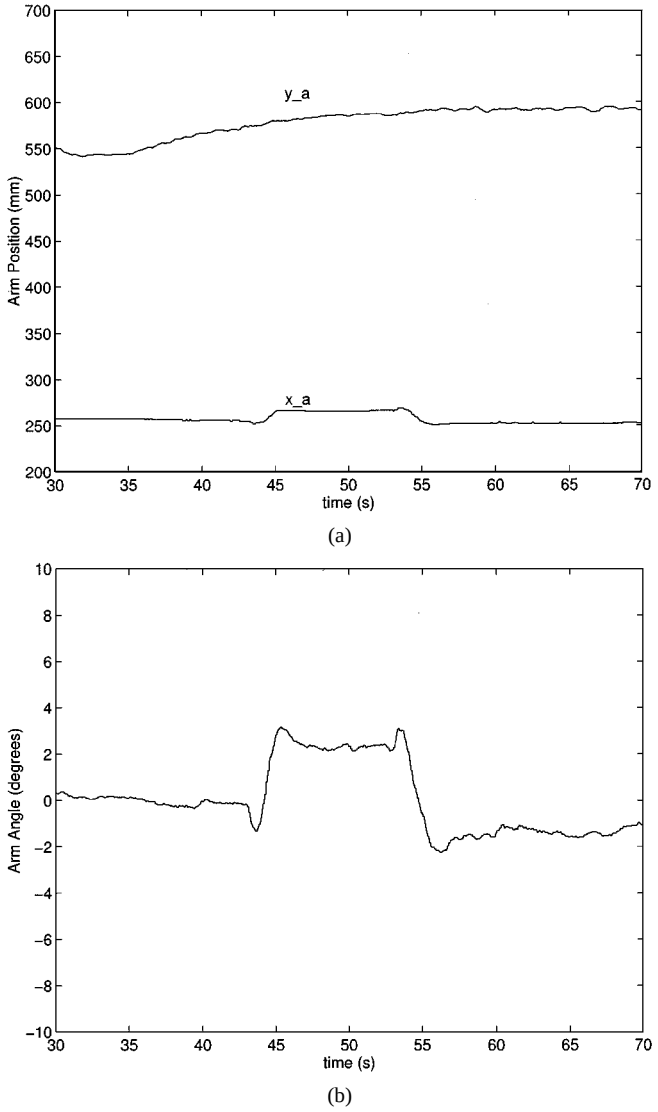

Fig. 7. Experiment 1: Positions (a) and orientation (b) of the active arm using a stiffness control law. Two robots are able to robustly carry a large object around a tight turn and the rear of the box only moves slightly as shown by the small deviations of the position of the actively controlled arm which is pressed against the box. The arm is controlled about the home position, $x_a = 254$ mm, $y_a = 568$ mm and $\theta_a = 0$.

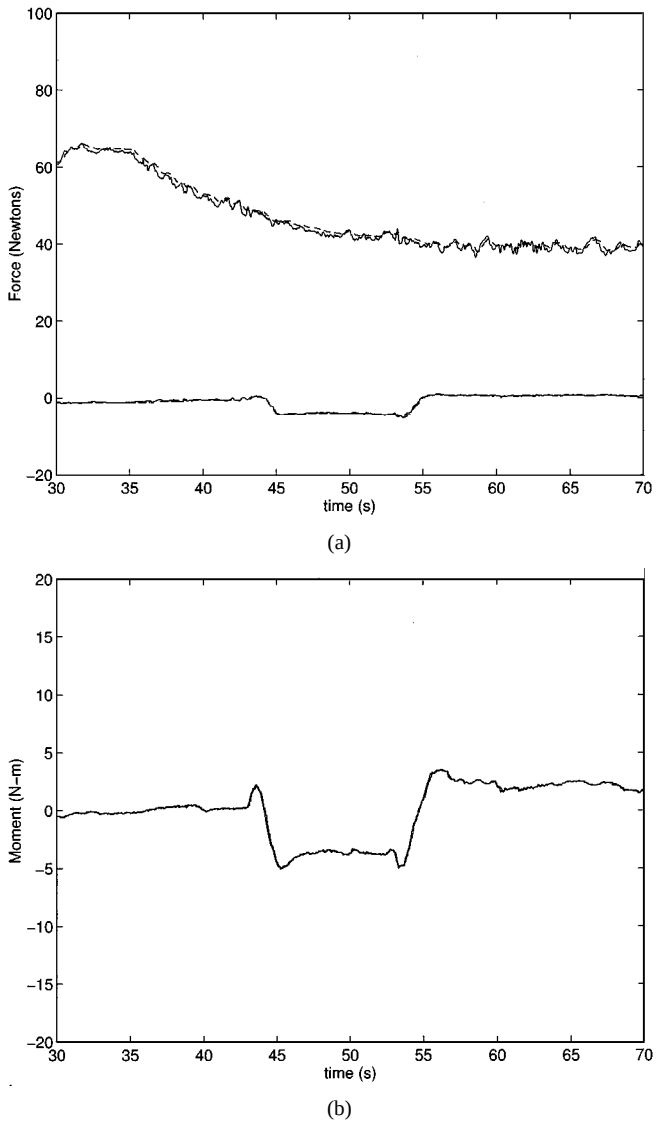

Fig. 8. Experiment 1: Forces (a) and moment (b) applied to the object with the arm controlled using a stiffness control law. Actual values are shown by a solid line while desired values are shown dashed. The actual forces and moment exactly mirror the position data achieving very good stiffness control with a desired, diagonal stiffness matrix.

with a desired force of $F_{x,des} = 0$, $F_{y,des} = 44$ N, and $M_{z,des} = 0$. The stiffness of the passive arm is dominated by the compliance of the grasped object and is estimated to be

$$K = \begin{pmatrix} 20000\ \frac{\text{N}}{\text{m}} & 0 & -14\,000\ \text{N} \\ 0 & 35\,000\ \frac{\text{N}}{\text{m}} & 0 \\ -14\,000\ \text{N} & 0 & 6500\ \text{Nm} \end{pmatrix}.$$

The variation of the active arm's position and orientation is shown in Fig. 7. In this experiment, the stiffness control law tries to keep the arm near the home position. The actual forces and moment applied by the arm to the object are given in Fig. 8.

In Experiment 2, the task is identical and the trajectories are therefore similar, but the arm on Robot 2 is controlled using a force control law with desired values of $F_x = 0$, $F_y = 44.48$ N and $M = 0$. The arm position and orientation is shown in Fig. 9. Comparing this to Fig. 7, it is clear that the angular variation of the arm is much greater than in the stiffness control case where restoring forces drive the arm toward the nominal orientation of zero degrees. However, from the force histories, it is evident that the forces and moment are held close to the desired values of $F_x = 0$, $F_y = 44.48$ N, and $M = 0$, even during the large position and orientation changes. However, the large orientation errors cause the object to be dropped in some cases.

In both experiments, the arm performed very well, either maintaining the desired stiffness or maintaining the desired forces throughout the experiment. Better performance is obtained when the active arm uses a stiffness control law because the arm stays close to the nominal position and the grasped object is centered between the platforms. In general, the stiffness control law is also more robust, especially with respect to initial position errors and with respect to errors that cause the two robots to drift.

B. Dynamic Reconfiguration of the Team

In Experiment 3, the experimental configuration is the same as in the previous two experiments [as shown in Fig. 1(a)]. The experiment illustrates how the labels R_1 and R_2 can be dynamically reassigned during the task. First, the the nonholonomic TRC platform is the leader, R_1. When the follower R_2, the Nomad XR4000, detects an obstacle that

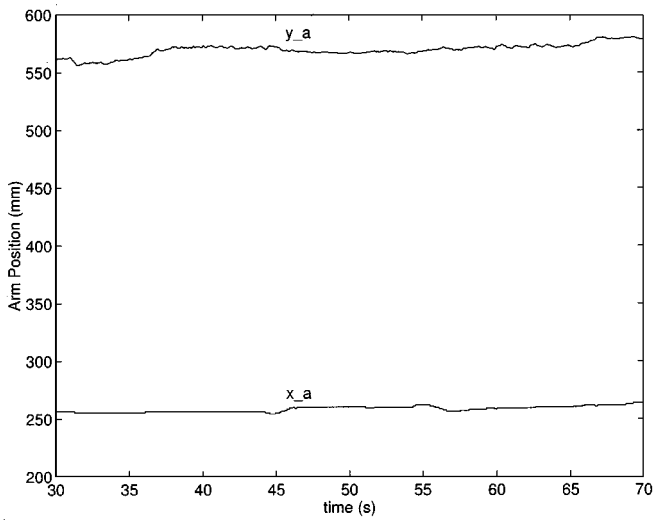

(a)

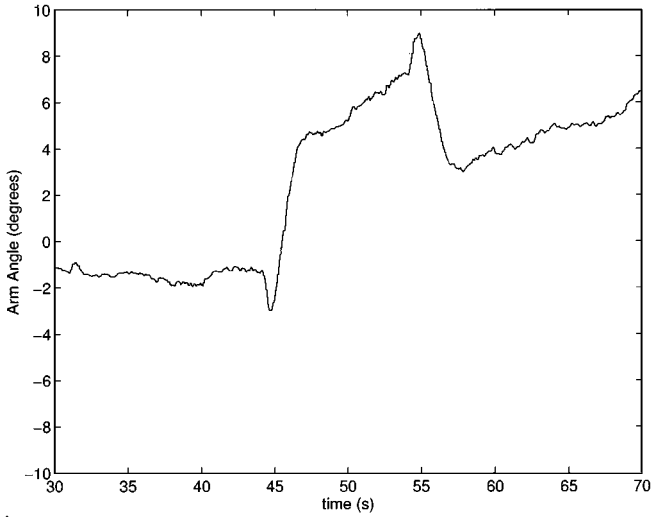

(b)

Fig. 9. Experiment 2: Positions (a) and orientation (b) of the active arm using a force control law. In this experiment, the angle of the box greatly deviates from the home position of zero degrees.

forces it to change its path, the follower sends a message asking to assume the role of the leader. The leader agrees and assumes the role of the follower. The leaders are changed and the ability of the robots to follow appropriate trajectories while maintaining the grasp is not affected through the transition. The flexibility in the control architecture is evident in this experiment.

There are three distinct stages in this experiment. Robot B (the TRC platform with the active arm) is initially the leader until Robot A, the follower, detects an obstacle that had not been detected and accounted for by the leader. The start and end of the first stage are labeled A and B for Robot B, respectively, and a and b for Robot A, respectively, in Fig. 10. Robot A gains control of the team and becomes the leader, until it passes the obstacle. The start and end of the second stage are labeled B and C, respectively, in Fig. 10. Then the lead platform regains control and plans a path back toward the original goal position. The start and end of the last stage are labeled C and D, respectively, in Fig. 10.

The trajectories are shown in Fig. 10. The system is able to carry the box even when the desired trajectories are changed abruptly when an obstacle is found. Because the arm position and orientation do not change very much during the experiment, the robots maintain a very tight distance between themselves even when the desired trajectory is changed twice.

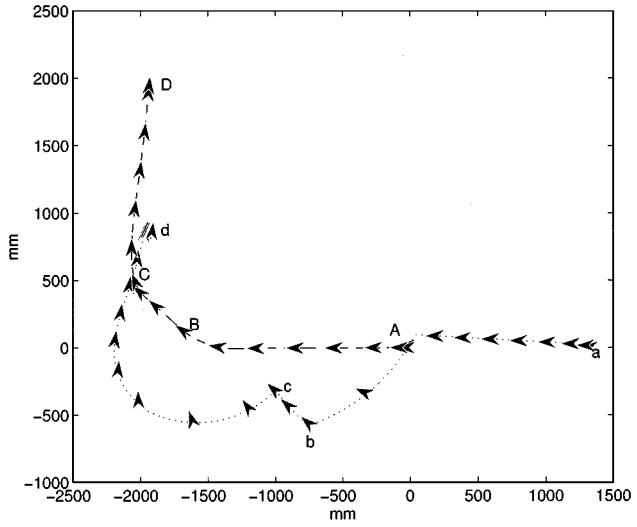

Fig. 10. The actual (dotted) path of Robot A and the actual (dashed) path of Robot B are shown for Experiment 3. Robot B goes through the intermediate positions A, B, C and D while the corresponding positions for Robot A are a, b, c and d.

C. Robustness to Positioning Errors

Experiments are performed to validate the use of the *look-ahead* controller described in Section II-C. The rear platform uses the look-ahead controller to adjust for alignment errors. Only the rear platform's trajectory is modified by the look-ahead controller. In our experimental results, we show that odometry errors, geometric errors as well as alignment errors can be corrected through this controller.

The Nomad robot is used as the lead robot, R_1 while the nonholonomic TRC platform with the actively controlled arm is used as the rear platform, R_2. In all trials, the Nomad robot and the TRC platform traverse along a straight path followed by a left turn. In the experimental plots, the ideal and commanded velocities for the trailing platform, R_2, the arm position compared to its nominal home position and the desired and actual position of the reference point on the arm (P and Q) are shown for different conditions.

In Experiment 4, the TRC platform is aligned with the Nomad robot, so the orientations of both platforms match perfectly. The commanded velocities match the ideal velocities. As shown in Fig. 11, the arm stays close to the nominal position. As per the terminology in Section II-C, the coordinates of the reference point Q, are $x_a = 254$ mm, $y_a = 568$ mm and $\theta_a = 0$. The actual position of the reference point on the arm is denoted by point P, with coordinates (p_1, p_2). It is clear that the desired and actual position (p_1, p_2) shown overlaid in Fig. 11 are virtually identical.

In Experiment 5, the estimate of the length, L is 1500 mm instead of 1360 mm, an error of more than 10 percent. The commanded velocities are significantly different from the ideal reference trajectory velocities. The accommodation by the actively controlled arm is shown in Fig. 12.

The look-ahead controller is able to correct for errors in misalignment between the two platforms and errors in the size of the box. In Experiment 5, even though the look-ahead controller significantly changes the commanded velocities, the performance of the arm is independently robust. It does not deviate significantly from its home position of $x_a = 254$ mm, $y_a = 568$ mm, and $\theta_a = 0$.

D. Coordination of Three Robots

In this section we present experimental results with the three platform configuration. The three platforms work cooperatively to transport the flexible board as shown in Fig. 1(b). The experiment demonstrates that we can control three robots and all are used to carry the

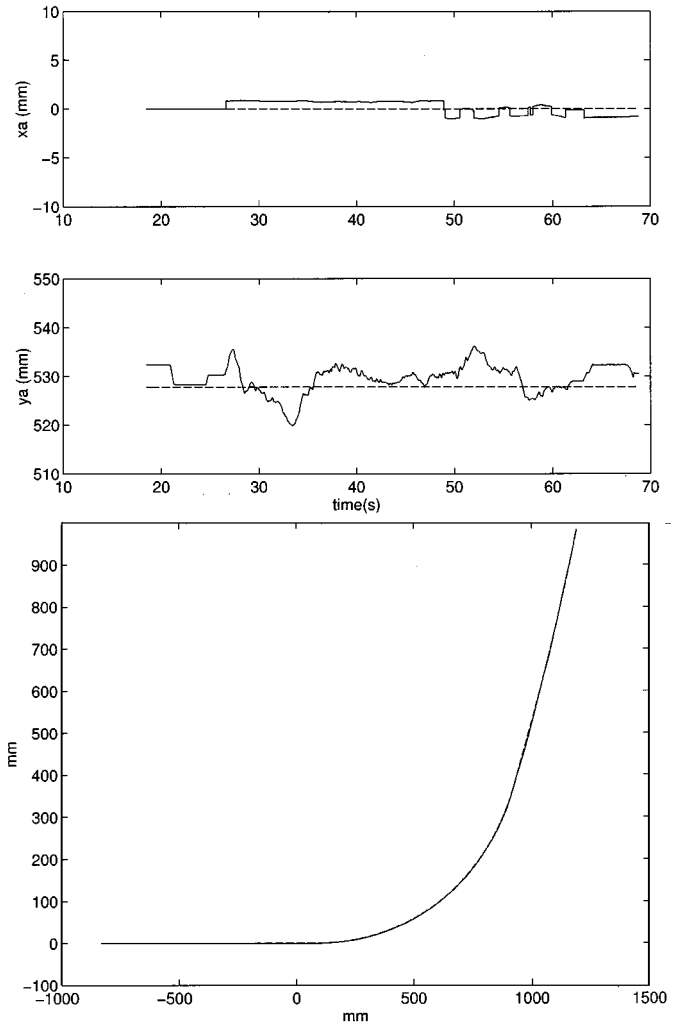

Fig. 11. Experiment 4: Because the arm remains close to its home position, the rear platform is aligned with the front platform. On the bottom, the desired position of the reference point Q (dashed) on the arm and the actual arm position P (solid) are overlaid.

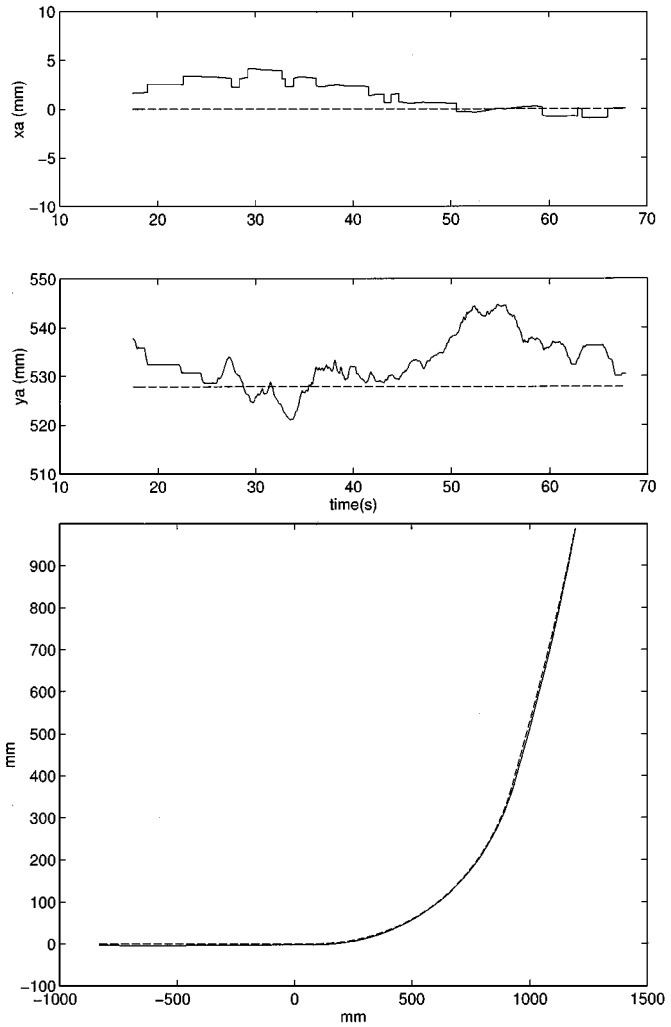

Fig. 12. Experiment 5: Even with the 10 percent error in the front platform's estimate of the length of the box, the arm still remains close to its home position. On the bottom, the desired position of the reference point Q on the arm (dashed) and the actual arm position P (solid) are overlaid. The addition of the *look-ahead* controller allows the system of robots to be robust to errors, not crushing or dropping the object while following difficult curved trajectories.

flexible board. A flexible board is chosen for two reasons. First, because it is flexible, a third robot is needed to support the board at the center. Secondly, the board is large and flimsy and tight coordination is needed; otherwise, it will bend and break.

The parameters governing the experiment are given below

$$\begin{aligned} f_{12} &= 4.45 \text{ N.}, \quad f_{13} = f_{23} = 0 \\ r_{12} &= 2315 \text{ mm.}, \quad \psi_{12} = 0, \\ r_{13} &= 1312 \text{ mm}, \quad r_{23} = 1355 \text{ mm}. \end{aligned}$$

and the stiffness matrices in metric units are estimated

$$K_1 = \begin{pmatrix} 20000 \frac{\text{N}}{\text{m}} & 0 & -16\,000 \text{ N} \\ 0 & 35\,000 \frac{\text{N}}{\text{m}} & 0 \\ -16\,000 \text{ N} & 0 & 7300 \text{ Nm} \end{pmatrix}$$

$$K_2 = \begin{pmatrix} 88 \frac{\text{N}}{\text{m}} & 0 & 0 \\ 0 & 175 \frac{\text{N}}{\text{m}} & 0 \\ 0 & 0 & 90 \text{ Nm} \end{pmatrix} \quad K_3 = (0) \qquad (11)$$

K_3 is zero because during the experiment, the robot simply supports the board and does not exert forces or moments in the plane.

The trajectory for the maneuver is shown in Fig. 13. The heading velocity for Experiment 6 is shown in Fig. 14. The heading velocity for the two nonholonomic platforms are labeled v_1 (lead platform) and v_2. The velocities in the x and y direction for the XR4000 are labeled v_x and v_y, respectively. The angular velocity for Experiment 6 is shown in Fig. 14. The angular velocity for the lead platform is labeled ω_1 and it is labeled ω_2 and ω_n for the two rear platforms.

Our experiments demonstrate that our architecture and control algorithms allow all three platforms to coordinate and cooperatively carry the flexible board.

V. Discussion

Using Robots A and B and a stiffness controller, we have shown robust performance in carrying an object over a distance of 6 m with 100% success. Using a force controller, internal forces and moment on the box are controlled, but success of the system is poor due to large orientation errors of the object as shown in Experiment 2.

In Experiment 3, the leader can be reconfigured multiple times, even though the platform and arm controllers are not changed. The decentralized structure allows the system to be organized differently during a task. In Experiments 4 and 5, the look-ahead controller improves the robustness of the system to numerous positioning errors due to odometry, acceleration and kinematic errors. Last, we demonstrated that three

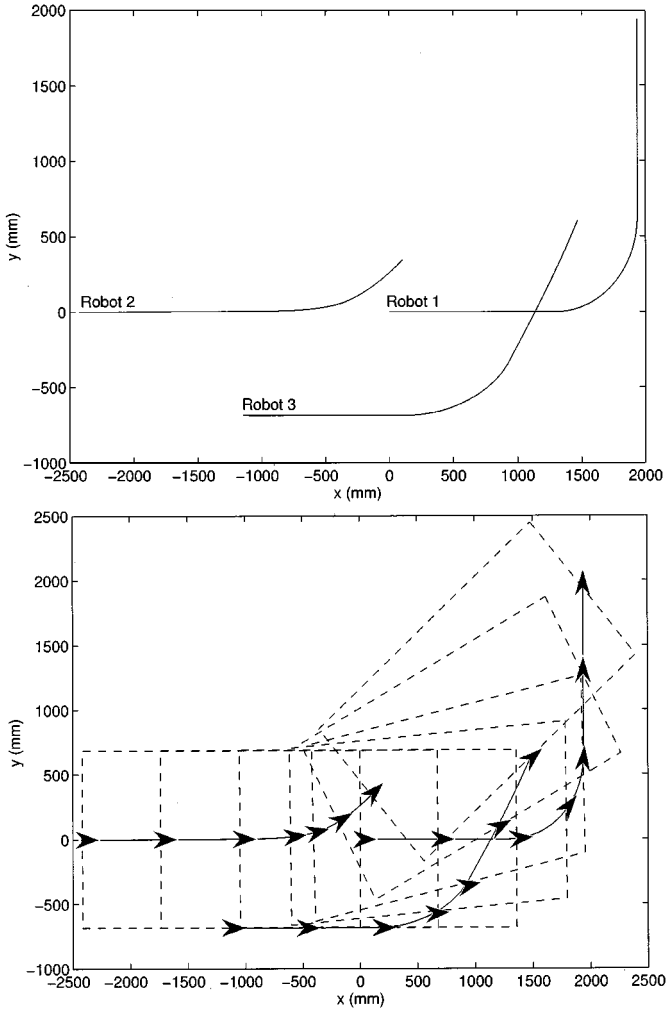

Fig. 13. Platform trajectories for the lead robot and follower robots while executing a turn. The board (dashed line) is carried by the three robots.

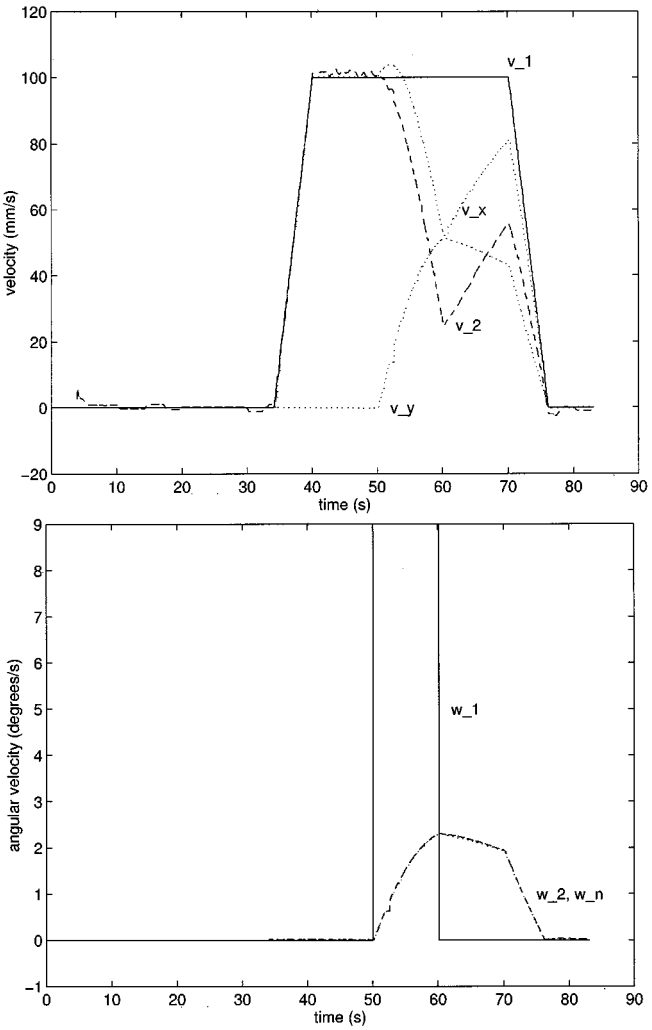

Fig. 14. Heading velocity for Experiment 6. The heading velocities for the two nonholonomic platforms are labeled v_1 (lead platform) and v_2. The velocities in the x and y direction for the XR4000 are labeled v_x and v_y, respectively. The angular velocity shown on the bottom for the lead platform is labeled ω_1. The angular velocities for the two rear platforms are equal and are labeled ω_2 and ω_n, respectively. ω_n is the angular velocity of the omnidirectional platform.

robots are able to transport a flimsy board. Coordination of three robots is much more difficult and two successful trials are presented from a set of ten trials.

In this paper, we have not focused on re-grasping, optimal placement and organization of multiple robots. It is clear that the compliance in the robot-object contacts plays an important role in determining grasp stability. A detailed analysis of this including a discussion on designing the compliance is presented in another paper [30].

VI. Conclusion

A flexible, scalable system is designed using multiple autonomous robots coordinated by a leader. We presented the control algorithms and the overall architecture for coordinating a small team of robots which can pick up, carry and lower objects of different sizes and masses. Additional robots can easily be added because each platform is controlled by independent sensors and controllers and it is the task specification that couples the robots. The architecture is flexible in the sense that it allows for the leaders to be dynamically reassigned during the execution of the task. A designated lead robot is responsible for task planning. Because the exchange of information is limited, the architecture scales reasonably well with the number of robots.

In our approach, the control of each platform is decomposed into the control of the gross trajectory and the control of the grasp. The two control problems are mechanically decoupled. As the platforms move, the force and position control problems are decoupled by allowing the position controlled robots to follow a desired path and by adding an active arm which controls the internal forces. One or more actively controlled, compliant arms control the grasp forces in the formation allowing the robot platforms to be position controlled. The excessive forces due to platform positioning errors and odometry errors are accommodated by the compliant arms.

We believe that these results will eventually lead to a truly flexible material handling system that will have a wide range of civilian and military applications.

References

[1] J. Adams, R. Bajcsy, J. Koczeka, V. Kumar, R. Mandelbaum, M. Mintz, R. Paul, C.-C. Wang, Y. Yamamoto, and X. Yun, "Cooperative material handling by human and robotic agents: Module development and system synthesis," *Expert Systems With Applications*, vol. 11, no. 2, 1996.

[2] T. Balch and R. C. Arkin, "Communication in reactive multiagent robotic systems," *Autonomous Robots*, vol. 1, no. 1, pp. 27–52, 1994.

[3] M. Mataric, "Reinforcement learning in the multi-robot domain," *Autonomous Robots*, vol. 4, no. 1, Jan. 1997.

[4] A. Agah and G. A. Bekey, "Autonomous mobile robot teams," in *Proc. of AIAA/NASA Conf. on Intelligent Robotics in Field, Factory, Service and Space (CIRFFSS'94)*, 1994, pp. 246–251.
[5] T. Balch and R. C. Arkin, "Behavior-based formation control for multi-robot teams," IEEE Trans. on Robotics and Automation, 1999, to be published.
[6] D. Rus, B. Donald, and J. Jennings, "Moving furniture with teams of autonomous robots," in *Proceedings of the 1995 IEEE/RSJ International Conference on Intelligent Robots and Systems*, 1995.
[7] C. R. Kube and H. Zhang, "Collective robotics: From social insects to robots," *Adaptive Behavior*, vol. 2, no. 2, pp. 189–219, 1993.
[8] D. Stillwell and J. Bay, "Toward the development of a material transport system using swarms of ant-like robots," in *Proc. 1993 Int. Conf. Robot. Automation*, Atlanta, GA, 1993.
[9] T. C. Hu, A. B. Kahng, and G. Robins, "Optimal robust path planning in general environments," *IEEE Trans. Robot. Automat.*, vol. 10, 1993.
[10] G. S. Sukhatme and G. A. Bekey, "An evaluation methodology for autonomous mobile robots for planetary exploration," in *In Proc. First ECPD Int. Conf. Advanced Robot. Intell. Automat.*, Athens, Greece, Sept. 1995, pp. 558–563.
[11] T. Sugar and V. Kumar, "Decentralized control of cooperating manipulators," in *Proc. 1998 Int. Conf. Robot. Automat.*, Belgium, 1998.
[12] M. Ahmadabadi and N. Eiji, "Constrain and move: A new concept to develop distributed object transferring protocols," in *Proc. 1997 Int. Conf. Robot. Automat.*, Albuquerque, NM, 1997.
[13] E. Paljug, X. Yun, and V. Kumar, "Control of rolling contacts in two-arm manipulation," *IEEE Trans. Robot. Automat.*, vol. 10, pp. 441–452, Aug. 1994.
[14] Y. Yamamoto and X. Yun, "Modeling and compensation of the dynamic interaction of a mobile manipulator," in *Proc. 1994 Int. Conf. Robot. Automat.*, CA, 1994.
[15] O. Khatib, K. Yokoi, K. Chang, D. Ruspini, R. Holmberg, A. Casal, and A. Baader, "Force strategies for cooperative tasks in multiple mobile manipulation systems," in *Int. Symp. Robot. Res.*, Munich, 1995.
[16] J. P. Desai and V. Kumar, "Nonholonomic motion planning for multiple mobile manipulators," in *Int. Conf. Robot. Automat.*, Albuquerque, NM, April 1997.
[17] T. Sugar and V. Kumar, "Multiple cooperating mobile manipulators," in *Proc. 1999 Int. Conf. Robot. Automat.*, Detroit, MI, 1999.
[18] S. D. Eppinger and W. P. Seering, "On dynamic models of robot force control," in *Proc. IEEE Int. Conf. Robot. Automat.*, Apr. 1986, pp. 29–34.
[19] T. Sugar and V. Kumar, "Design and control of a compliant parallel manipulator for a mobile platform," in *Proc. 1998 ASME Design Eng. Tech. Conf. Comput. Eng. Conf.*, Atlanta, GA, 1998.
[20] J. P. Desai, V. Kumar, and J. P. Ostrowski, "Control of changes in formation for a team of mobile robots," in *Proc. 1999 Int. Conf. Robot. Automat.*, Detroit, MI, May 1999.
[21] T. Sugar, J. P. Desai, V. Kumar, and J. P. Ostrowski, "Coordination of multiple mobile manipulators," in *Proc. 2001 Int. Conf. Robot. Automat.*, 2001.
[22] J. K. Salisbury, "Kinematics and Force Analysis of Articulated Hands," Ph.D., Stanford Univ., CA, 1982.
[23] V. D. Nguyen, "Constructing force-closure grasps," *Int. J. Robot. Research*, vol. 7, no. 3, pp. 3–16, 1988.
[24] J.-C. Latombe, *Robot Motion Planning*. Boston, MA: Kluwer Academic, 1991.
[25] M. Žefran, J. P. Desai, and V. Kumar, "Continuous motion plans for robotic systems with changing dynamic behavior," in *2nd Int. Workshop on Algorithmic Foundations of Robotics*, Toulouse, France, 1996.
[26] T. Sugar, "Design and Control of Cooperative Mobile Robotic Systems," Ph.D., The Univ. Pennsylvania, PA, 1999.
[27] "XR4000," Nomadic Technologies Inc., Mountain View, CA, 1999.
[28] "RangeLAN2 7100 ISA Card," Proxim, Mountain View, CA , 1999.
[29] T. Sugar and V. Kumar, "Coordination of multiple mobile platforms for manipulation and material transport," in *Video Proc. IEEE Int. Conf. Robot. Automat.*, Detroit, MI, 1999.
[30] ——, "Metrics for analysis and optimization of grasps and fixtures," in *Proc. 2000 Int. Conf. Robot. Automat.*, 2000.

An Improved Inverse Kinematic and Velocity Solution for Spatial Hyper-Redundant Robots

Farbod Fahimi, Hashem Ashrafiuon, and C. Nataraj

***Abstract*—A new and efficient kinematic position and velocity solution scheme for spatial hyper-redundant manipulators is presented. The manipulator's arm has discrete links and universal joints. Backbone curve concepts and a modal approach are used to resolve the manipulator's redundancy. The effects of the mode shapes and the slope of the backbone curve at the starting point on the workspace are studied. It is shown that the usage of conventional mode shapes limits the workspace of the hyper-redundant arm. By introducing new mode shapes, an improved workspace is obtained. A simple and efficient recursive fitting method is introduced to avoid complications involved with solving systems of nonlinear algebraic equations. This method also guarantees the existence of solutions for the inverse kinematic problem at the velocity level. Velocity properties of the backbone curve are investigated and the inverse velocity propagation is solved for the spatial hyper-redundant arm. The velocity propagation scheme is recursive and is efficiently applicable to any number of links.**

***Index Terms*—Backbone curve, hyper-redundant, inverse kinematics, modal approach, robot workspace.**

I. Introduction

Hyper-redundant manipulators have many more kinematic degrees of freedom than the number of task space coordinates. Therefore, the classical methods cannot be used for solving their inverse kinematics. Many investigations have focused on the redundancy resolution of this type of manipulator based on the manipulator Jacobian pseudo-inverse [1]. Singularity avoidance [2], [3], obstacle avoidance [4]–[6], and keeping joint variables in their physical limitation [1] are some examples of supplementary tasks. Extended Jacobian inverse [3] and augmented inverse Jacobian [7] are also utilized extensively. In the case of spatial hyper-redundant manipulators with hundreds of degrees of freedom, the computational burden of pseudo-inverse Jacobian becomes prohibitive, despite proposed improvements [8]. Furthermore, most of the proposed schemes handle the inverse kinematic problem at the velocity level only.

The modal approach has been presented as a unique method for redundancy resolution of hyper-redundant manipulators in [9]. In this method, a backbone curve is defined as a piecewise continuous curve that captures the important macroscopic geometric features of a hyper-redundant robot. The backbone curve is restricted by a set of intrinsic shape functions to a modal form. The mode shape functions are arbitrary and lead to an efficient inverse kinematics solution at the position level. Once the backbone curve is determined for an assumed location of the end-effector, depending on the physical implementation morphology of a particular manipulator, various fitting algorithms can be developed. This method has been utilized to form the foundation for obstacle avoidance [10], locomotion [11], and motion control [12], [13]. Some researchers have shown the application of the modal ap-

Manuscript received June 19, 2001; revised October 8, 2001. This paper was recommended for publication by Associate Editor S. Chiaverini and Editor A. De Luca upon evaluation of the reviewers' comment. This work was supported by Concurrent Technologies Corporation's (CTC's) National Applied Software Engineering Center (NASEC) program, which is aponsored by the Defense Advanced Research Projects Agency (DARPA).

The authors are with the Department of Mechanical Engineering, Villanova University, Villanova, PA 19085 USA (e-mail: farbod.fahimi@villanova.edu; hashem.ashrafiuon@villanova.edu; c.nataraj@villanova.edu).

Publisher Item Identifier S 1042-296X(02)01812-8.